As originally published in the SMTA Proceedings.

CHARACTERIZATION OF HYBRID CONFORMAL COATINGS USED FOR MITIGATING TIN WHISKER GROWTH

Junghyun Cho[1], Stephan J. Meschter[2], Suraj Maganty[1], Dale Starkey[3], Mario Gomez[3], David G. Edwards[3], Abdullah Ekin[4], Kevin Elsken[4], Jason Keeping[5], Polina Snugovsky[5], and Jeff Kennedy[5]

[1]Binghamton University (SUNY)
Binghamton, NY, USA
jcho@binghamton.edu

[2]BAE Systems
Endicott, NY, USA

[3]Henkel Electronic Materials LLC
Irvine, CA, USA

[4]Bayer MaterialScience LLC
Pittsburgh, PA, USA

[5]Celestica Inc.
Toronto, ON, Canada

ABSTRACT

A conformal coating of polyurethane (PU) consisting of hard and soft segments is being studied in an effort to prevent tin whisker penetration. For this, the coating needs to possess optimum mechanical properties by providing sufficient strength, modulus, and hardness while maintaining good ductility and toughness. Typical monolithic PU films, however, do not possess all these required properties, so silica nanoparticles are incorporated into a PU film to improve its whisker mitigation effectiveness. In the present work, nanoparticles were functionalized to bind them to the polymer structure while avoiding the agglomeration among the particles. Selection of the ideal concentration of nanoparticles is determined by establishing microstructure–property relations. Structural features at different length scales are characterized by various instruments including atomic force microscope (AFM) and scanning electron microscope (SEM) while mechanical properties are evaluated via macroscopic tensile testing as well as nanoindentation. In particular, the nanoindentation testing emulates the whisker penetration behavior by producing local deformation of PU around an indenter tip.

Key words: Pb-free, tin whisker, conformal coatings, nanoparticles, polyurethane, nanoindentation

INTRODUCTION

Pb-free electronics using tin-based solders and pure tin are seriously exposed to a risk of tin whisker growth that can result in electrical failure [1-5]. In an effort to mitigate such failure, conformal coatings can be used to provide an efficient means of blocking the tin whisker growth [6-8]. These coatings have been used for environmental protection for electronics components, so can serve a dual purpose. Some literature has indeed shown that a conformal coating over the surfaces where whisker growth is pronounced can either slow down the whisker growth rate or trap the whiskers [8,9]. To serve as an effective mitigation, the coating needs to be thick enough to minimize the risk of the whisker penetration [9]. Its coverage is also important to ensure protection of the whole whisker prone surface because the thinner coating regions exhibit greater whisker penetration and will be the weakest link [6]. Furthermore, coating properties need to be optimized to provide the protection without coating failure. These properties include elastic modulus, yield strength, tensile strength, hardness, toughness, and elongation. Coating adhesion to the surface will be important not only for whisker mitigation but also the reliability of the overall packaging system. Several polymer coatings have been investigated for this purpose, which include acrylic, urethane, their hybrid, silicone, and parylene coatings [8]. There are, however, no conclusive outcome yet as to which coatings and what types of properties should be selected.

Conformal coatings can be applied via various techniques; select spray, atomized spray, dip and/or vapor deposition. A key process variable is the viscosity formulation. Both select and atomized spray methods apply their coatings via a lineof-sight application, thus limiting their coverage beneath large components; e.g., ball grid arrays (BGAs). By dipping or submerging the assembly, the coverage is improved, as the line-of-site is not a factor and more of the metallic surfaces get covered, but heavy build-up that is susceptible to cracking during thermal cycling can occur. Vapor deposition used for parylene coating has excellent coverage over all exposed surfaces, thereby providing a uniform, thin coating application. However, this solution is cost prohibitive and difficult to rework in the field because specialized equipment is needed. The eventual goal is to develop a liquid PU coating application method that obtains improved coverage, reduced variation and has good manufacturability/repairability.

In this work, we have synthesized a conformal polyurethane coating consisting of hard (hexamethylene di-isocyanate) and soft (polyol) segments. The microphase size and crosslinking of the PU chain are responsible for the unique properties observed in these polymers [10]. Moreover, nanoparticles from silica or alumina can be incorporated to further improve its whisker mitigation effectiveness. Agglomeration, non-uniform distribution, and void defects that often occur with increasing concentration of nanoparticles have to be avoided to maximize the efficiency of nanoparticles. Not only for avoiding agglomeration, nanoparticles were functionalized also to bind them to the PU structure. One purpose of this study is to select the optimum concentration of nanoparticles based upon microstructural observation and associated mechanical properties that can effectively mitigate the tin whisker growth. Structural features at nanometer scales are characterized by high-resolution imaging instruments including AFM and SEM while mechanical properties are evaluated via macroscopic tensile testing as well as nanoindentation. In particular, the depth-sensitive nanoindentation testing can emulate the whisker penetration behavior by examining local deformation of PU around an indenter tip. This work will also highlight coating properties that are of importance in resisting the tin whisker growth.

PREPARATION OF CONFORMAL COATINGS

Conformal coatings were prepared by mixing PU base resin with a nanoparticle suspension. PU resin system was chosen because it can be formulated to have a wide range of liquid viscosity and solid physical properties. Base PU chemistry systems have already been qualified for IPC-CC830 and MIL-I-46058 and can withstand exposure to RTCA/DO-160 fluids like JP-8 jet fuel and Skydrol® vapors. Moisture curable solvent-based polyurethane (PC18M, from Henkel) was employed in this study. The silica nanoparticles were dispersed in a hexamethylene diisocyanate (HDI) system (Desmodur® XP2742, from Bayer MaterialScience) that is chemically compatible with the base PU systems. The nanosilica particle diameter distribution in the Desmodur® XP2742 is D50 = 14.5 and D90 = 20.8 nanometers (note: D50 and 90 represent the 50th and 90th percentile diameters, respectively).

The nanoparticles in the suspension were functionalized with a silane-modified isocyanate to crosslink with the polymer chains in the base systems. As shown in Figure 1, the particle isocyanate functionalization results in nanoparticles which are covalently bonded to the polymer backbone, thus coupling the inorganic and organic materials (i.e., silica and polymer) [11]. High-speed dispersion or sonication was employed to facilitate particle dispersion in the suspension medium.

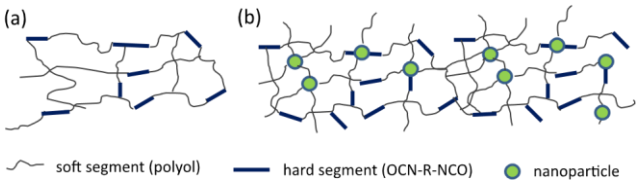

Figure 1. Schematic of post-reaction mixture between a base resin and a particle suspension: (a) basic polyurethane; (b) polyurethane with nanoparticle reinforcement.

The three types of samples were utilized in the current evaluation were (1) coatings on printed circuit board coupons (see Fig. 2), (2) coatings on glass microscope slides and (3) cast coatings formed on a glass substrate. The liquid coatings were deposited with a plastic pipet along an edge of the printed circuit boards or the glass slides and a grooved steel mandrel was used to spread the coating to a thickness of 20 to 40 □m. The coatings on the glass microscope slides were used for the AFM measurements, some of the nanoindentation measurements and after being peeled off used for the cross-section examination. The rectangular shaped sheet coating samples used for the tensile testing were cast on a glass substrate. The thickness of the cast film was controlled using two shims to set the height of a squeegee blade that was drawn across the deposited liquid coating to obtain a thickness ranging from 100 to 330 □m. All samples were air dried for a minimum of 30-45 minutes and then cured for a minimum of two hours at 60 ºC (140 ºF) in an oven having a minimum relative humidity of 30 percent in accordance with the PC18M datasheet. The tensile test and the cross-section samples were peeled from glass substrates after curing.

Figure 2. Printed circuit board coupon 101 mm x 69 mm x 1.2 mm thick.

RESULTS AND DISCUSSION

Microstructure Observation of Polyurethane Coatings

Figure 3 shows a top-view AFM image of unfilled PU coatings, where a 'wormy' network band and several island protrusions (< 100 nm in lateral dimension) are observed. The latter features seem to be related to 'bubble' formation during coating deposition. Some structural features are more clearly explained in the AFM phase contrast image as shown in Fig. 3 (b). In this image, those protrusions are not detectable as they are part of the polymer network, but the two contrasting areas are observed. Those network bands shown in the height image give 'dark' contrast while the dimples inside the bands are shown as 'bright' contrast. Based upon this observation, this network structure appears to be a hard segment which wraps around the soft segment. This conclusion can also be supported from high-resolution SEM images, which will be explained later.

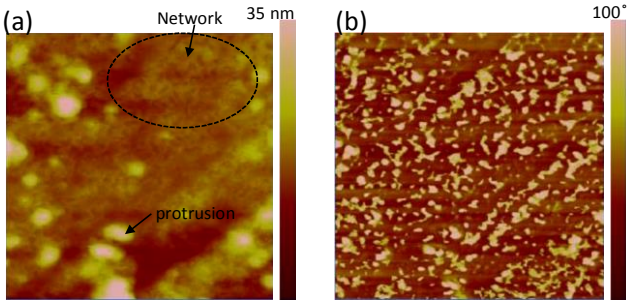

Figure 3. AFM images of unfilled polyurethane coatings (in 1 □m x 1 □m): (a) height image; (b) phase image.

The PC18M base resin was mixed with the coating suspension (from 10% to 50%), where both nonfunctionalized (Cab-O-Sil™ TS610 particles in suspension) and functionalized nanosilica particles (in XP2742) were employed. It is shown that functionalized silica particles are essential to avoid agglomeration as shown in Fig. 4. PU coatings with non-functionalized SiO_2 exhibited a strong agglomeration behavior (in some cases, over 200 □m in size) while the functionalized nanoparticle-filled coating did not show any apparent agglomeration behavior when compared at similar concentrations of about 15 wt% SiO_2containing PU coatings.

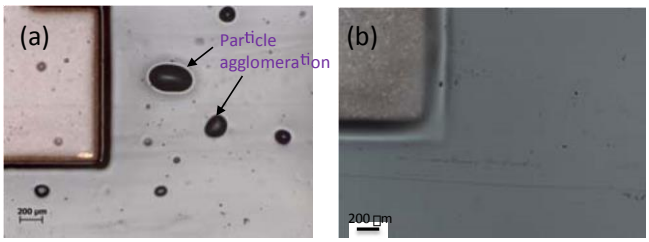

Figure 4. Optical images of polyurethane coatings with (a) 14.6 wt.% non-functionalized SiO_2; (b) 15.2 wt.% functionalized SiO_2.

Mechanical Behavior of Polyurethane Coatings

After adding nanoparticles to the PU base resin, mechanical properties of filled PU coatings were improved as shown in Fig. 5. Both elastic modulus and nanohardness increased after 10% XP2742 SiO_2 (which corresponds to 3.5 wt% SiO_2). These properties decreased with indentation depth, which is a typical behavior of moisture-cured polymers. Nanosilica-filled PU coatings displayed lower hardness values near the surface region (< 500 nm range). Mechanical properties of those nanosilica-filled PU coatings, however, did not show any improvement with 30% XP2742 addition (corresponding to 9.8 wt% SiO_2) or 50% XP2742 addition (to 15.2 wt% SiO_2). In fact, there was a decrease as seen in the modulus of 30% XP2742 case due to its more dependence on indentation depth.

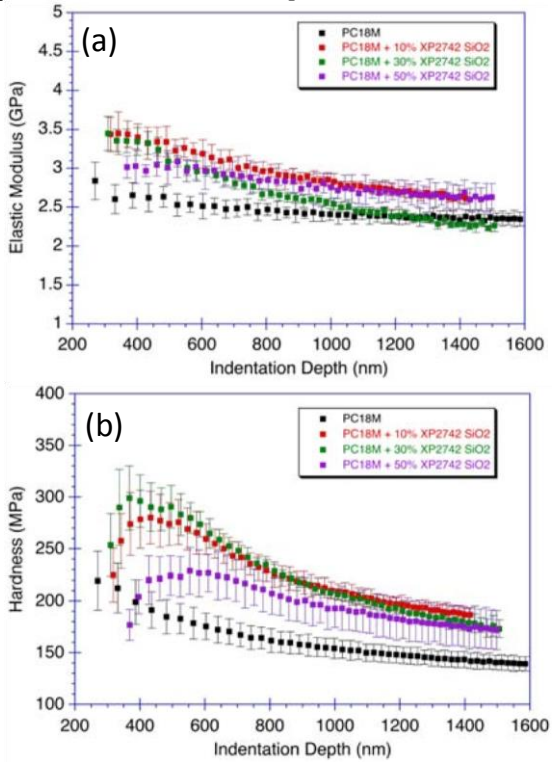

Figure 5. Nanoindentation of polyurethane coatings with different amounts of SiO_2: (a) elastic modulus; (b) nanohardness.

While nanoindentation data represent local deformation behavior near the surface of the PU coatings, tensile testing

results assess the bulk behavior of nanosilica-filled PU coatings. Table 1 shows tensile properties of filled PU, as compared to those of unfilled PU. The tensile specimen was 2.5 inch x 0.5 inch cut from the cast material with a gauge length of 0.5 inch. Testing was performed on an Instron instrument with a displacement control of 0.1 inch/min. Large sample-to-sample variation was observed partly due to the void defect population embedded during the sheet casting process. As was the case for the nanoindentation test, PU coating with 30% XP2742 or more exhibited a decrease in modulus and strengths. The 50% XP2742 case was rather brittle, thereby showing a limited total elongation. This brittleness resulted from the bubble defects that existed in the PU sheets.

Table 1. Tensile properties of nanosilica-filled PU coatings

	PC18M	**PC18M + 10% XP2742**	**PC18M + 30% XP2742**	**PC18M + 50% XP2742**
wt.% of SiO_2	0	3.5	9.8	15.2
E (GPa)	1.0 ± 0.06	1.1 ± 0.26	0.68 ± 0.03	0.68 ± 0.06
Y.S. (MPa)	47 ± 7	56 ± 12	32 ± 8	39 ± 6
T.S. (MPa)	48 ± 9	54 ± 14	32 ± 9	39 ± 6
Total El. (%)	65 (avg), 134 (max)	65 (avg); 97 (max)	78 (avg); 138 (max)	33 (avg); 100 (max)

(E: Young's modulus; Y.S.: yield strength; T.S.: tensile strength at break; El.: elongation)

Examination of ruptured PU films after tensile testing indicates the failure origin at the bubbles (or voids) as shown in Fig. 6. These defect locations provide a stress concentration site, where the crack initiates and propagates. Shear bands also extend from this location with about 45˚ angle from a tensile loading axis. Because of the presence of these defects, there was premature failure, as well as data scattering. It ultimately made the polymer film quite brittle. Therefore, it will be necessary to have the defect concentration reduced to increase a ductility, which can be comparable to that of the parylene film.

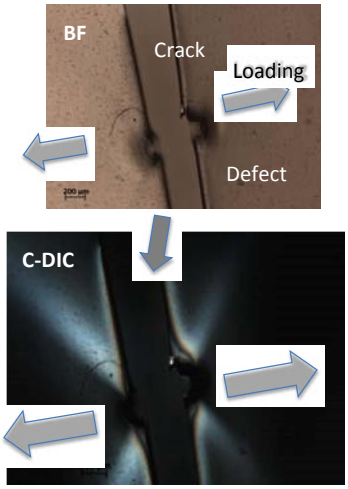

Figure 6. A crack grown from a defect site embedded in PU film: (a) bright field optical micrograph; (b) Cdifferential interference contrast (DIC) image. Arrows indicate tensile loading direction.

Effect of Nanosilica on Polyurethane Microstructures

Figure 7 shows top view AFM image of a PU coating with the 50% XP2742 SiO_2. SiO_2 nanoparticles are shown here and gathered together to create small agglomerated particle regions less than 100 nm in some cases. Since the agglomeration tendency increased with increasing particle concentration, increased attention to particle uniformity is needed at elevated concentrations to have mechanical consistent behavior.

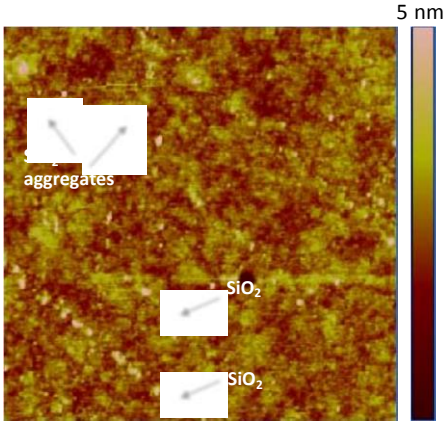

Figure 7. AFM image of the PU coating with 50% XP2742 SiO_2 (15.2 wt% SiO_2). The whole view is in 5 x 5 □m.

In order to see the nanoparticle distribution more clearly, cross-sectional samples were prepared by freezing the freestanding films (peeled from glass slides) in liquid nitrogen, fracturing by bending force, and etching with Ar ions, followed by Cr coating to prevent sample charging during field emission SEM operation at 2 kV.

Figure 8 shows cross-sectional images of the PU coating with 30% XP2742 SiO_2. Nanosilica particle concentration was highest toward the bottom of the film (adjacent to the glass

slide before the sample was peeled off) as compared to the top side of the coating. The observed nanoparticle size was ~ 20 nm which is consistent with the initial particle data (D90=20 nm). The fact that few nanosilica particles were observed at the top layer may explain why the nanoindentation testing did not show dramatic increase in mechanical properties with increasing particle concentration because the indentation testing is done on the top surface

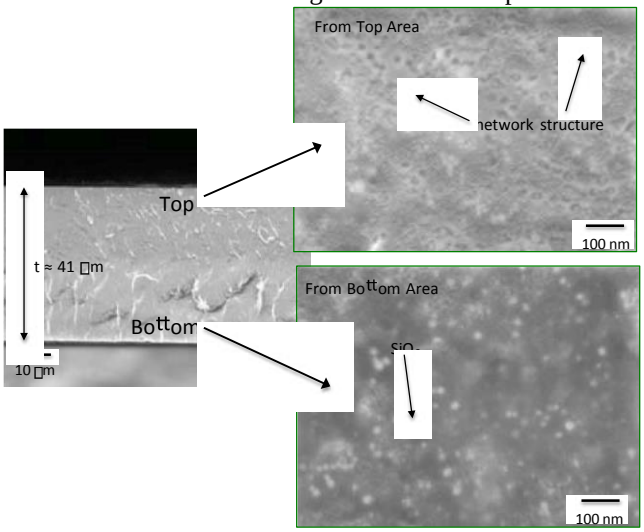

Figure 8. Cross-sectional SEM image of PU coating with 30% XP2742 SiO_2 (9.8 wt% SiO_2).

area. Like unfilled PU coatings, this coating shows dimpled network structure, but the nanosilica particles are mostly found in non-network regions. It indicates the presence of functionalized nanoparticle can disrupt the original PU network or lower the degree of phase separation [12]. The degree of phase separation has been shown to influence mechanical properties of segmented PU [13]. Therefore, it will potentially influence tin whisker mitigation behavior, and mechanical properties of these microstructure variations will need further investigation.

Given that the presence of nanoparticle influences the original network structure of PU coatings, the present work compares the cross-sectional images of three different concentrations of XP2742 SiO_2 (10%, 30%, and 50%). The aforementioned network structure for unfilled PU coating is also shown in 10% XP2742 SiO_2 case (Fig. 9 (a)), where the dimpled region with surrounding network structure is shown. It was not easy to locate the presence of nanoparticles at such low concentration (3.5 wt%). With the increased SiO_2 content (9.8 wt.%), two contrasting regions were observed (Fig. 9 (b)); one with more nanosilica, where network structure appeared to be destroyed (that is, creating smooth regions), and the other with the dimpled network structure, which is close to that of unfilled PU or PU with low concentrations. The network bands were shown to be thinner. With a further increase of SiO_2 content (15.2 wt%), a clean cleaved surface for cross-sectional imaging was more difficult to obtain even after freezing the PU samples (Fig. 9 (c)). This resulted in more charging in SEM operation, so the image contrast was poorer than the other two PU samples. The band structure seemed to become finer at this level of nanosilica addition.

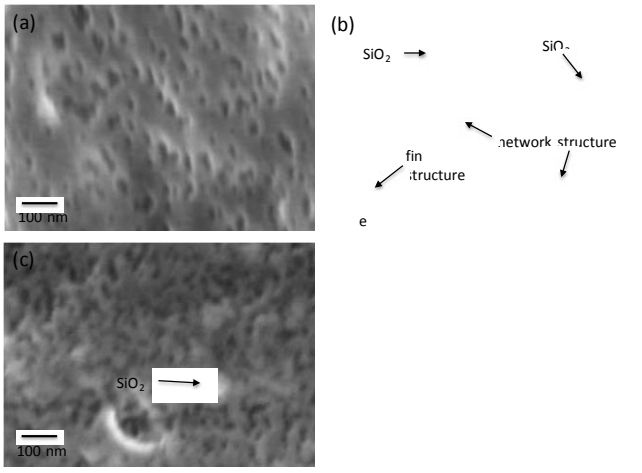

Figure 9. Cross-sectional SEM images of PU coatings with (a) 10% XP2742 SiO_2, (b) 30% XP2742 SiO_2, and (c) 50% XP2742 SiO_2.

CONCLUSIONS

Functionalized nanosilica particles approximately 20 nm in diameter were added to a PU coating in an attempt to attain its optimum mechanical properties for mitigating tin whisker growth. It was shown that mechanical properties do not continuously increase with the nanosilica concentration. This was due to non-uniform distribution of nanosilica and polymer structure change with added nanoparticles. Phase separation also seemed to be affected by the presence of nanosilica. In particular, microdefects created during film processing are responsible for film brittleness and limited ductility. Establishment of the structure – property relationship is essential to identify optimal microstructures of the nanoparticle-filled PU, which can be of importance in tin whisker mitigation.

FUTURE WORK

Future work will involve more characterization using the tools such as cryo-transmission electron microscopy to observe the particle distribution and agglomeration behavior more clearly. In addition, chemical structure, bonds, and functionality of PU coatings will be examined via Fourier transform infrared spectroscopy. Mechanical properties of key microstructures will be evaluated using the nanoindentation system, along with AFM. Other nanoparticles (e.g., nanoalumina) and other types of PU base resin (e.g., UV-cured) will also be investigated. The potential of PU coatings for tin whisker mitigation will be evaluated by comparing its performance with that of common conformal coatings such as parylene.

ACKNOWLEDGMENTS

This research was sponsored by the Strategic Environmental Research and Development Program (SERDP) of

Department of Defense. We would like to acknowledge the Analytical and Diagnostics Lab (ADL) at Small Scale Systems Integration and Packaging (S^3IP) Center for the SEM and AFM work. In addition, we acknowledge Dr. InTae Bae and Daniel VanHart at S^3IP of SUNY Binghamton for providing help for specimen preparation.

REFERENCES

[1] "Tin Whiskers and Conversion to Pb-Free," *Circuits Assembly*, **16** [12], 38-40 (2005).

[2] G. T. Galyon, "Annotated tin whisker bibliography and anthology," *IEEE Transactions on Electronics Packaging Manufacturing*, **28 [1]** [1], 94-122 (2005).

[3] T. King-Ning, S. Jong-ook, W. Albert Tzu-Chia, N. Tamura, and T. Chih-Hang, "Mechanism and prevention of spontaneous tin whisker growth," *Materials Transactions*, **46** [11], 2300-2308 (2005).

[4] S. Mathew, M. Osterman, M. Pecht, and F. Dunlevey, "Evaluation of Pure Tin Plated Copper Alloy Substrates for Tin Whiskers," *Circuits World*, **35 [1]**, 3-8 (2009).

[5] J. W. Osenbach, "Tin whiskers: An illustrated guide to growth mechanisms and morphologies," *JOM*, **63** [10], 57-60 (2011).

[6] S. Han, M. Osterman, S. Meschter, and M. Pecht, "Evaluation of Effectiveness of Conformal Coatings as Tin Whisker Mitigation," *J. Electron. Mater.*, **41 [9]**, (2012).

[7] T. A. Woodrow and E. A. Ledbury, "Evaluation of Conformal Coatings as a Tin Whisker Mitigation Strategy," in *Proceedings of the IPC/JEDEC 8th International Conference on Lead-Free Electronic Components and Assemblies*. (San Jose, CA, 2005), 2005.

[8] T. A. Woodrow and E. A. Ledbury, "Evaluation of Conformal Coatings as a Tin Whisker Mitigation Strategy, Part II," in *Proceedings of the The Proceedings of SMTA International Conference*. (Rosemont, IL, 2006), 2006.

[9] L. Panashchenko, J. Brusse, and H. Leidecker, "Long Term Investigation of Urethane Conformal Coating Against Tin Whisker Growth," in *Proceedings of the IPC Tin Whisker Conference*. 2010), 2010.

[10] L.-C. Xu, P. Soman, J. Runt, and C. A. Siedlecki, "Characterization of Surface Microphase Structures of Poly(urethane Urea) Biomaterials by Nanoscale Indentation with AFM," *J. Biomater. Sci. Polymer Edn.*, **18 [4]**, 353-368 (2007).

[11] O. Pyrlik, A. Nennemann, and R. Maleika, "Nanoparticle-modified Coating Raw Materials for High Performance PU Coatings." In *Eurocoat 2009***.** Barcelona, Spain.

[12] Z. S. Petrovic, Y. J. Cho, I. Javni, S. Magonov, N. Yerina, D. W. Schaefer, J. Ilavsky, and A. Waddon, "Effect of Silica Nanoparticles on Morphology of Segmented Polyurethanes," *Polymer*, **45 [12]**, 42854295 (2004).

[13] K. Nakamae, T. Nishino, S. Asaoka, and Sudaryanto, "Microphase separation and surface properties of segmented polyurethane--Effect of hard segment content," *International Journal of Adhesion and Adhesives*, **16** [4], 233-239 (1996).